Studies of the 5′-Substituted Phenylisoquinoline-Based Iridium Complexes Using Density Functional Theory

Cheng-Hsien Yang, Wei-Lin Su, Kai-Hung Fang, Shao-Pin Wang,* and I-Wen Sun*

Department of Chemistry, National Cheng Kung University, Tainan, Taiwan, 701, Republic of China

Received April 11, 2006

To examine the effects of coordination sites and the nature of ligands reported for color-tuning of a few cyclometalated Ir(III) complexes, a series of 3′-substituted (F, CH_3, OCH_3, and CF_3) phenylisoquinoline (piq) ligands were synthesized and successfully used to prepare iridium complexes, including bis[1-(5′-methyl)phenylisoquinolinato-*N*,$C^{2'}$]iridium(III) (acetylacetonate) (**6a1**), bis[1-(5′-trifluoromethyl)phenylisoquinolinato-*N*,$C^{2'}$]iridium(III) (acetylacetonate) (**6a2**), bis[1-(5′-methoxy)phenylisoquinolinato-*N*,$C^{2'}$]iridium(III) (acetylacetonate) (**6a3**), and bis[1-(5′-fluoro)phenylisoquinolinato-*N*,$C^{2'}$]iridium(III) (acetylacetonate) (**6a4**). Density functional theory results indicate that two conflicting effects, electronic and steric, can be applied to account for the substitution-sensitive coordination sites of piq: the methoxyl- or fluoro-substituted ligand generates both 2′-coordinated and 6′-coordinated isomers. Coordination of methoxy substitution prefers 6′-coordination of piq dominated by steric effects, while coordination of fluoro substitution prefers 2′-coordination, arising from better back-donation of the iridium center. Correlations of HOMO−LUMO gaps with electroluminescence (EL) data are discussed. More importantly, the EL data are well predicted by time-dependent density functional theory calculations.

1. Introduction

The mixing of singlet and triplet excited states by doping phosphorescent dyes into a charge-transporting host as emissive layers greatly enhances the internal phosphorescence quantum efficiency of organic light-emitting diodes (OLEDs) toward 100%. Among the various reported triplet emitters including complexes of Ir(III), Pt(II), Ru(II), and Os(II), the iridium complexes appear to be the most promising for OLED applications.[1] A famous class of red phosphorescent emitters using phenylisoquinoline-based iridium complexes has been extensively studied.[2] These studies show that the photophysical properties of the cyclometalated iridium complexes can be finely tuned by systematic control of the nature and position of the substituents on the ligands. In the studies, the substitution on the meta-position of the phenyl ring appeared to be interesting because isomers of iridium complexes (in addition to the 5′-substituted compound) could often be obtained depending on the substituents. For example, while Laskar et al.[3] obtained a 2′-coordinated 2-phenylbenzthiazole iridium complex with the F substituent (Ir(3-Fbt)$_2$(acac)) because the steric hindrance is small, Grushin et al.[4] obtained 6′-coordinated phenylpyrindine iridium complexes with the relatively larger CF_3 and OCH_3 subsitituents, probably due to steric hindrance. However, Lee et al.[5] obtained both 2′-coordinated and 6′-coordinated phenylpyridazine iridium complexes with the OCH_3 substituent despite its steric hindrance. These results could not be ascribed simply to the steric effect, and the molecular orbitals of the iridium complexes must also be considered.

In recent years, approaches using density functional theory (DFT) techniques have received large acceptance for their predictions of the ground and excited states in organometallic molecules.[6] These research activities inspired us to initiate a study to observe the color tuning of a series of highly efficient red iridium phosphorescent emitters based on the 3′-substituted phenylisoquinoline (piq) ligands with different substituents. In this paper, calculations using DFT techniques were applied to interpret the different behavior of these substituents.

2. Experimental Section

General Information and Materials. Scheme 1 outlines how the phenylisoquinoline ligands were synthesized and utilized for preparing a series of iridium complexes. All starting materials were purchased from Aldrich and TCI and were used without further purification. ^{1}H NMR and ^{13}C NMR spectra were measured in CD_2Cl_2 solution on a Bruker Avance-300 (300 MHz), AMX-400 (400 MHz), or Avance-500 (500 MHz) NMR spectrometers with tetramethylsilane (TMS) as the internal standard. The EI-mass spectra were recorded on a Bruker APEX II. Melting points were measured using a capillary melting point apparatus. HRMS spectra were obtained using a MAT-95XL high-resolution mass spectrometer. Elemental analyses have been carried out by using an Elementar vario EL III analyzer.

---

* Corresponding authors. Tel: +886-6-2757575-65355; +886-6-275757575-65354. Fax: +886-6-2740552. E-mail: iwsun@mail.ncku.edu.tw; spwang@mail.ncku.edu.tw.

(1) (a) Lamansky, S.; Djurovich, P.; Murphy, D.; Abdel-Razzaq, F.; Lee, H.; Adachi, C.; Burrows, P. E.; Forrest, S. R. *J. Am. Chem. Soc.* **2001**, *123*, 4304. (b) Brooks, J.; Babayan, Y.; Lamansky, S.; Djurovich, P. I.; Tsyba, I.; Bau, R.; Thompson, M. E. *Inorg. Chem.* **2002**, *41*, 3055. (c) Wu, P. C.; Yu, J. K.; Song, Y. H.; Chi, Y.; Chou, P. T.; Peng, S. M.; Lee, G. H. *Organometallics* **2003**, *22*, 4938. (d) Tung, Y. L.; Wu, P. C.; Liu, C. S.; Chi, Y.; Yu, J. K.; Hu, Y. H.; Chou, P. T.; Peng, S. M.; Lee, G. H.; Tao, Y.; Carty, A. J.; Shu, C. F.; Wu, F. I. *Organometallics* **2004**, *23*, 3745.

(2) (a) Okada, S.; Iwawaki, H.; Furugori, M.; Kamatani, J.; Igawa, S.; Moriyama, T.; Miura, S.; Tsuboyama, A.; Takiguchi, T.; Mizutani, H. *SID 02 Digest* **2002**, 1360. (b) Huang, Y. T.; Chuang, T. H.; Shu, Y. L.; Kuo, Y. C.; Wu, P. L.; Yang, C. H.; Sun, I. W. *Organometallics* **2005**, *24*, 6230.

(3) Laskar, I. R.; Chen, T. M. *Chem. Mater.* **2004**, *16*, 111.

(4) Grushin, V. V.; Herron, N.; LeCloux, D. D.; Marshall, W. J.; Petrov, V. A.; Wang, Y. *Chem. Commun.* **2001**, 1494.

(5) Lee, S. J.; Lee, J. S.; Hwang, K. J.; Kim, Y. K.; Kim, Y. S.; Park, N. G.; Shin, E. J.; Lee, S. H. *Curr. Appl. Phys.* **2005**, *5*, 43.

(6) (a) Becke, A. D. *J. Chem. Phys.* **1993**, *98*, 5648. (b) Casida, M. E.; Jamorski, C. K.; Casida, C.; Salahub, D. R. *J. Chem. Phys.* **1998**, *108*, 4439. (c) Hay, P. J. *J. Phys. Chem. A* **2002**, *106*, 1634. (d) Li, H. C.; Chou, P. T.; Hu, Y. H.; Cheng, Y. M.; Liu, R. S. *Organometallics* **2005**, *24*, 1329.

10.1021/om060323p CCC: $33.50

Scheme 1. Synthesis of Iridium Complexes

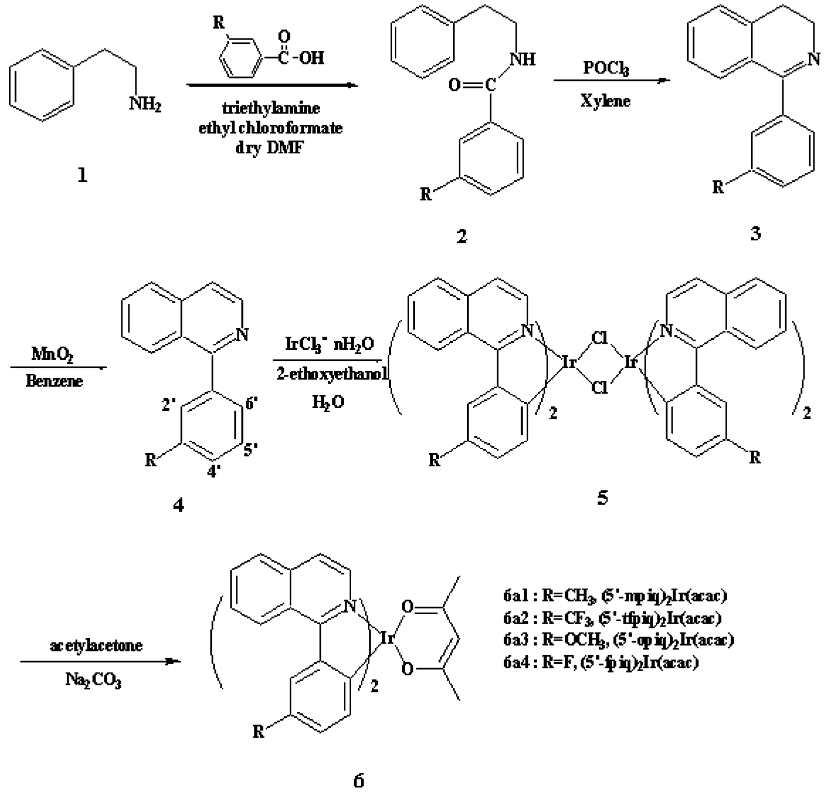

Synthesis of 1-(3′-Methyl)phenylisoquinoline (4a1). 4a1 was prepared by a modified method (Scheme 1). First, 3-methyl-*N*-phenethylbenzamide (**2**) was synthesized and introduced with a cyclization process to obtain 1-*m*-tolyl-3,4-dihydroisoquinoline (**3**). After deprotonation of **3**, the white solid product was obtained in a 37.26% yield, mp = 73.0−75.8 °C. EI-MS: *m*/*z* 218, $[M]^+$. ^1H NMR ($CDCl_3$, 300 MHz): δ 8.60 (d, J = 5.6 Hz, 1H), 8.11 (d, J = 8.2 Hz, 1H), 7.86 (d, J = 8.2 Hz, 1H), 7.68 (m, 2H), 7.47 (m, 4H), 7.30 (d, J = 5.6 Hz, 1H), 2.46 (s, 3H).

Synthesis of 1-(3′-trifluoromethyl)phenylisoquinoline (4a2): yellow oil. Yield: 49.36%. EI-MS: *m*/*z* 273, $[M]^+$. ^1H NMR ($CDCl_3$, 300 MHz): δ 8.46 (d, J = 5.4 Hz, 1H), 7.95 (s, 1H), 7.83 (d, J = 7.5 Hz, 1H), 7.72 (d, J = 7.5 Hz, 1H), 7.46 (t, J = 7.5 Hz, 2H), 7.45 (m, 3H), 7.31 (t, J = 5.4 Hz, 1H).

Synthesis of 1-(3′-methoxy)phenylisoquinoline (4a3): yellow oil. Yield: 13.23%. EI-MS: *m*/*z* 234, $[M]^+$. ^1H NMR ($CDCl_3$, 400 MHz): δ 8.59 (d, J = 5.7 Hz, 1H), 8.10 (d, J = 7.7 Hz, 1H), 7.81 (d, J = 8.2 Hz, 1H), 7.61 (m, 2H), 7.48 (t, J = 7.7 Hz, 1H), 7.42 (t, J = 5.7 Hz, 1H), 7.26 (m, 2H), 7.03 (d, J = 7.7 Hz, 1H), 3.48 (s, 3H).

Synthesis of 1-(3′-fluoro)phenylisoquinoline (4a4): yellow oil. Yield: 14.18%. EI-MS: *m*/*z* 223, $[M]^+$. ^1H NMR ($CDCl_3$, 300 MHz): δ 8.59 (d, J = 5.7 Hz, 1H), 8.06 (d, J = 8.2 Hz, 1H), 7.86 (d, J = 8.2 Hz, 1H), 7.66 (m, 2H), 7.50 (m, 4H), 7.20 (m, 1H).

Synthesis of bis[1-(5′-methyl)phenylisoquinolinato-*N*,$C^{2'}$]-iridium(III) (acetylacetonate) (6a1). The cyclometalated Ir(III) μ-chloro-bridged dimers were synthesized by the method reported by Nonoyama.[7] 1-(3′-Methyl)phenylisoquinoline (10.0 mmol) and 0.4 equiv of $IrCl_3{\cdot}H_2O$ (Next Chimica) were heated in a 3:1 mixture of 2-ethoxyethanol and water. This slurry was heated at 100 °C for 24 h. After cooling to room temperature, the precipitate was filtered off and washed with deionized water. The solid obtained was placed in a flask and dispersed in 2-ethoxyethanol. Acetylacetone and sodium carbonate were added to the solution, and the mixture was heated at 126 °C for 15 h. After cooling to room temperature, the crude product was filtered off and washed with deionized water, followed by two portions of *n*-hexane and ether. The solid was dried, and column chromatography was used to give red pure product **6a1** in 15.53% yield. EI-MS: *m*/*z* 728, $[M]^+$. HRMS: found *m*/*z* 728.2019, calcd for $C_{37}H_{31}IrN_2O_2$ M, 728.2015. ^1H NMR (CD_2Cl_2, 300 MHz): δ 9.02 (m, 2H), 8.43 (d, J = 6.4 Hz, 2H), 8.09 (s, 2H), 7.97 (m, 2H), 7.74 (m, 4H), 7.51 (d, J = 6.4 Hz, 2H), 6.52 (d, J = 7.8 Hz, 2H), 6.21 (d, J = 5.5 Hz, 2H), 5.32 (s, 1H), 2.28 (s, 6H), 1.79 (s, 6H). ^{13}C NMR (CD_2Cl_2, 75 MHz): δ 174.9, 159.0, 137.4, 136.9, 130.7, 127.4, 123.4, 120.8, 120.6, 120.1, 119.7, 117.9, 117.4, 116.9, 116.5, 110.1, 90.6, 18.5, 11.2. Anal. Calcd for $C_{37}H_{31}IrN_2O_2{\cdot}H_2O$: C, 59.58; H, 4.46; N, 3.76. Found: C, 60.06; H, 4.53; N, 3.64.

Synthesis of bis[1-(5′-trifluoromethyl)phenylisoquinolinato-*N*,$C^{2'}$]iridium(III) (acetylacetonate) (6a2): dark red solid. Yield: 34.26%. FAB-MS: *m*/*z* 836, $[M]^+$. HRFABMS: found *m*/*z* 836.1452, calcd for $C_{37}H_{25}F_6IrN_2O_2$ M, 836.1450. ^1H NMR (CD_2Cl_2, 300 MHz): δ 8.94 (m, 2H), 8.44 (m, 4H), 8.04 (m, 2H), 7.83 (m, 4H), 7.65 (d, J = 6.3 Hz, 2H), 6.87 (d, J = 7.8 Hz, 2H), 6.49 (d, J = 8.0 Hz, 2H), 5.32 (s, 1H), 1.79 (s, 6H). ^{13}C NMR (CD_2Cl_2, 75 MHz): δ 175.5, 157.6, 147.7, 137.4, 130.4, 127.6, 124.1, 121.5, 118.9, 117.8, 116.6, 116.1, 115.7, 115.0, 114.9, 113.0, 112.6, 111.6, 90.9, 21.8, 18.4. Anal. Calcd for $C_{37}H_{25}F_6IrN_2O_2$: C, 53.15; H, 3.01; N, 3.35. Found: C, 53.59; H, 3. 53; N, 3.13.

Synthesis of bis[1-(5′-methoxy)phenylisoquinolinato-*N*,$C^{2'}$]-iridium(III) (acetylacetonate) (6a3): dark red solid. Yield: 10.08%. EI-MS: *m*/*z* 760, $[M]^+$. HREIMS: found *m*/*z* 760.1918, calcd for $C_{37}H_{31}IrN_2O_4$ M, 760.1913. ^1H NMR (CD_2Cl_2, 500 MHz): δ 8.98 (m, 2H), 7.77 (m, 8H), 7.40 (d, J = 6.1 Hz, 2H), 7.16 (d, J = 6.1 Hz, 2H), 6.76 (d, J = 8.4 Hz, 2H), 6.58 (d, J = 8.4 Hz, 2H), 5.32 (s, 1H), 1.79 (s, 6H), 1.53 (s, 6H). ^{13}C NMR (CD_2Cl_2, 125 MHz): δ 157.4, 144.2, 144.0, 135.8, 130.1, 127.3, 126.8, 120.4, 117.9, 117.3, 116.8, 110.8, 106.7, 106.2, 19.9. Anal. Calcd for $C_{37}H_{31}IrN_2O_4$: C, 58.46; H, 4.11; N, 3.69. Found: C, 58.25; H, 4.62; N, 3.37.

Synthesis of bis[1-(5′-fluoro)phenylisoquinolinato-*N*,$C^{2'}$]iridium(III) (acetylacetonate) (6a4): dark red solid. Yield: 67.95%. EI-

---

[7] Nonoyama, M. *Bull. Chem. Soc. Jpn.* **1974**, *47*, 767.

Table 1. Relative Energies, MO Energies, Band Gaps, and T_1 Energies Obtained for Iridium Complexes

complex	E_{rel} (kJ/mol)[a]	HOMO (eV)	LUMO (eV) (%)[b]	band gap (eV)	T_1(calcd) (eV)[c]	EL(exptl) (eV)[d]	atomic charge[e]		
							Ir	N	$C^{2'}$
(5′-mpiq)$_2$Ir(acac)	0.0	−4.68	−1.78 (2.4)	2.90	1.97	1.94	0.90	−0.58	−0.20
(3′-mpiq)$_2$Ir(acac)	37.8	−4.71	−1.76 (3.1)	2.95	2.04		0.93	−0.57	−0.24
(5′-tfpiq)$_2$Ir(acac)	0.0	−5.27	−2.15 (2.1)	3.12	2.14	2.07	0.93	−0.58	−0.20
(3′-tfpiq)$_2$Ir(acac)	38.2	−5.12	−1.86 (2.4)	3.25	2.19		0.94	−0.58	−0.22
(5′-opiq)$_2$Ir(acac)	0.0	−4.44	−1.78 (2.2)	2.66	1.80	1.88	0.90	−0.58	−0.20
(3′-opiq)$_2$Ir(acac)	11.4	−4.50	−1.59 (3.0)	2.92	2.02		0.95	−0.56	−0.30
(5′-fpiq)$_2$Ir(acac)	11.9	−4.85	−2.00 (2.4)	2.86	1.94	1.97	0.91	−0.58	−0.20
(3′-fpiq)$_2$Ir(acac)	0.0	−4.89	−1.78 (2.7)	3.11	2.14		0.94	−0.57	−0.33

[a] Relative energies are the difference between the total energies of the 3′- and 5′-isomers, with the lower energy set to zero. [b] Values in parentheses are iridium 5d-orbital content mixed into the LUMO given in percentage (5d-characters). [c] Carried out by TDDFT calculations. [d] Device structure: ITO/NPB (50 nm)/CBP: 6% dopant (30 nm)/BCP (10 nm)/AlQ3 (30 nm)/LiF (1 nm)/Al. [e] From Mulliken population analysis.

Table 2. Crystallographic Data of (3′-fpiq)$_2$Ir(acac)

formula	$C_{35}H_{25}F_2IrN_2O_2$
fw	735.77
space group	$P2_1/c$
a/Å	10.7643(4)
b/Å	18.1469(8)
c/Å	14.5661(7)
β/deg	105.504(2)
V/Å^3	2741.8(2)
Z	4
no. of reflns measd	21 038
no. of indep reflns	4844 [$R_{(int)} = 0.1323$]
no. of params	374
final R ($I > 2\sigma(I)$)	$R_1{}^a = 0.0812$, $wR_2{}^b = 0.1727$
goodness of fit on F^2	1.120

[a] $R_1 = \sum|F_o| - |F_c|/\sum|F_o|$. [b] $wR_2 = [\sum w[(F_o{}^2 - F_c{}^2)^2]/\sum[w(F_o{}^2)^2]]^{1/2}$. $w = 1/\sigma^2(F_o{}^2) + (0.075P)^2]$, where $P = [\max(F_o{}^2,0) + 2F_c{}^2]/3$.

Table 3. Selected Bond Lengths (Å) and Angles (deg) for (3′-fpiq)$_2$Ir(acac)

Ir(1)−C(15)	1.993(19)	Ir(1)−C(30)	1.988(17)
Ir(1)−N(1)	2.053(13)	Ir(1)−N(2)	2.045(12)
Ir(1)−O(1)	2.133(11)	Ir(1)−O(2)	2.168(12)
N(1)−C(9)	1.340(2)	N(1)−C(1)	1.360(2)
N(2)−C(24)	1.340(2)	N(2)−C(16)	1.350(2)
C(15)−Ir(1)−C(30)	92.2(6)	C(15)−Ir(1)−N(1)	80.4(7)
C(30)−Ir(1)−N(1)	98.9(6)	C(15)−Ir(1)−N(2)	99.2(7)
C(30)−Ir(1)−N(2)	79.7(6)	N(1)−Ir(1)−N(2)	178.5(5)

MS: m/z 736, $[M]^+$. HREIMS: found m/z 736.1523, calcd for $C_{37}H_{31}F_2IrN_2O_2$ M, 736.1513. ^1H NMR (CD_2Cl_2, 400 MHz): δ 8.92 (m, 2H), 8.44 (d, J = 6.5 Hz, 2H), 8.01 (d, J = 8.0 Hz, 2H), 7.97 (m, 2H), 7.75 (m, 4H), 7.52 (d, J = 6.5 Hz, 2H), 6.50 (m, 2H), 6.50 (m, 2H), 5.32 (s, 1H), 1.80 (s, 6H). 2′-Coordination isomer: ^1H NMR (CD_2Cl_2, 400 MHz) δ 9.00 (m, 2H), 8.38 (d, J = 6.5 Hz, 2H), 8.16 (d, J = 8.0 Hz, 2H), 7.95 (m, 2H), 7.76 (m, 4H), 7.49 (d, J = 6.5 Hz, 2H), 6.98 (m, 2H), 6.38 (m, 2H), 5.32 (s, 1H), 1.74 (s, 6H).

X-ray Structural Analysis. A crystal of (3′-fpiq)$_2$Ir(acac) was obtained from solutions of CH_2Cl_2−hexane. The crystal data were selected for indexing and intensity data collection on a Siemens SMART CCD diffractometer equipped with a normal focus, 3 kW sealed tube X-ray source at 200 K. No significant decay was observed for all samples during the data collection. Data were process on a PC using the Bruker AXS SHELXTL NT software package. Neutral atom scattering factors were taken from Cromer and Waber. The crystal of (3′-fpiq)$_2$Ir(acac) belongs to the monoclinic space group $P2_1/c$. All structures were solved by direct methods. All non-hydrogen atoms were refined anisotropically. The positions for all hydrogen atoms were either calculated or located directly from difference Fourier maps, and their contributions in the structural factor calculation were included. The crystallographic data of (3′-fpiq)$_2$Ir(acac) are given in Table 2, and selected bond lengths and angles are summarized in Table 3.

Computational Methodology. The ground-state geometries of the iridium complexes were optimized by DFT (B3LYP) [8] calculations using the Gaussian 98 software package. [9] Double-ζ quality plus polarization function basis sets were employed for all of the ligands (6-31G*) and Ir (LANL2DZ). A relativistic effective core potential (ECP)[10] on Ir replaced the inner core electrons, leaving the outer core $[(5s)^2(5p)^6]$ electrons and the $(5d)^6$ valence electrons of Ir(III). Atomic charges relevant to our discussions obtained by Mulliken population analysis are available. Time-dependent density functional theory (TDDFT)[11] calculations were also performed with the B3LYP functional at the same basis set level under optimized ground-state geometries to get excited-state energies, which give a vertical excitation (Franck−Condon principle) approach that could be comparable to experimental data.

3. Results and Discussion

Scheme 1 shows the synthesis process for the ligands and the iridium complexes. After deprotonation of **3**, a series of analogous ligands including 1-(3′-methyl)phenylisoquinoline (**4a1**), 1-(3′-trifluoromethyl)phenylisoquinoline (**4a2**), 1-(3′-methoxy)phenylisoquinoline (**4a3**), and 1-(3′-fluoro)phenylisoquinoline (**4a4**) were obtained and characterized. The desired iridium complexes **6aX** (**X** = 1, 2, 3, 4) were synthesized from the above ligands and characterized by ^1H NMR, ^{13}C NMR, mass spectrometry, and high-resolution spectrometry.

The experimental data indicated that the type of iridium complexes produced in this study was affected by the substituents. For either methyl- or trifluoromethyl-substituted phenylisoquinolines (**4a1** and **4a2**), only the 6′-coordinated (5′-mpiq)$_2$Ir(acac) (**6a1**) and (5′-tfpiq)$_2$Ir(acac) (**6a2**) were obtained, as expected by steric effects. Values of relative energy (E_{rel}) of the two iridium stereoisomers, energy differences between the pair of isomers arising from the two different coordination sites, have been calculated. The CH_3- or CF_3-substituted ligands give a 6′-coordinated isomer lower in energy than the 2′-coordinated isomer by 37.8 or 38.2 kJ/mol, as presented in Table 1.

For methoxyl-substituted ligands, **4a3**, or fluoro-substituted ligands, **4a4**, however, the 2′-coordinated and the 6′-coordinated

---

(8) (a) Becke, A. D. *J. Chem. Phys.* **1993**, *98*, 5648. (b) Lee, C.; Yang, W.; Parr, R. G. *Phys. Rev. B* **1988**, *37*, 785.

(9) Frisch, M. J.; et al. *Gaussian 98*, Revision A.11; Gaussian, Inc.: Pittsburgh, PA, 2001.

(10) Hay, P. J.; Wadt, W. R. *J. Chem. Phys.* **1985**, *82*, 270.

(11) (a) Stratmann, R. E.; Scuseria, G. E.; Frisch, M. J. *J. Chem. Phys.* **1998**, *109*, 8218. (b) Bauernschmitt, R.; Ahlrichs, R. *Chem. Phys. Lett.* **1996**, *256*, 454. (c) Casida, M. E.; Jamorski, C.; Casida, K. C.; Salahub, D. R. *J. Chem. Phys.* **1998**, *108*, 4439.

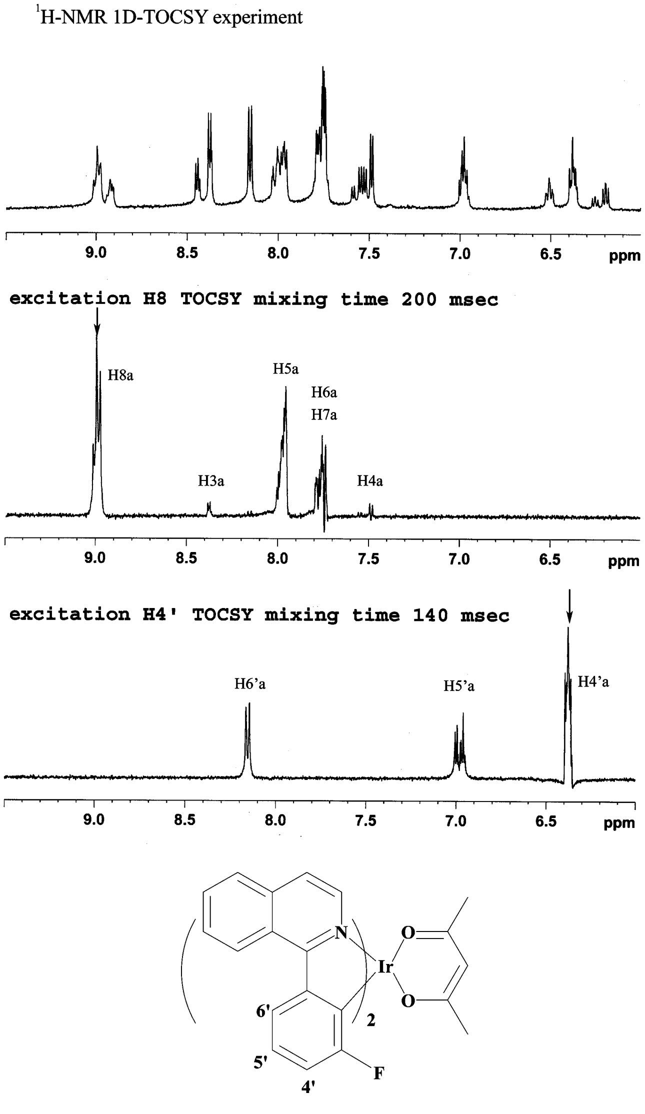

Figure 1. ^{1}H NMR 1D-TOSCY for (3′-fpiq)$_2$Ir(acac).

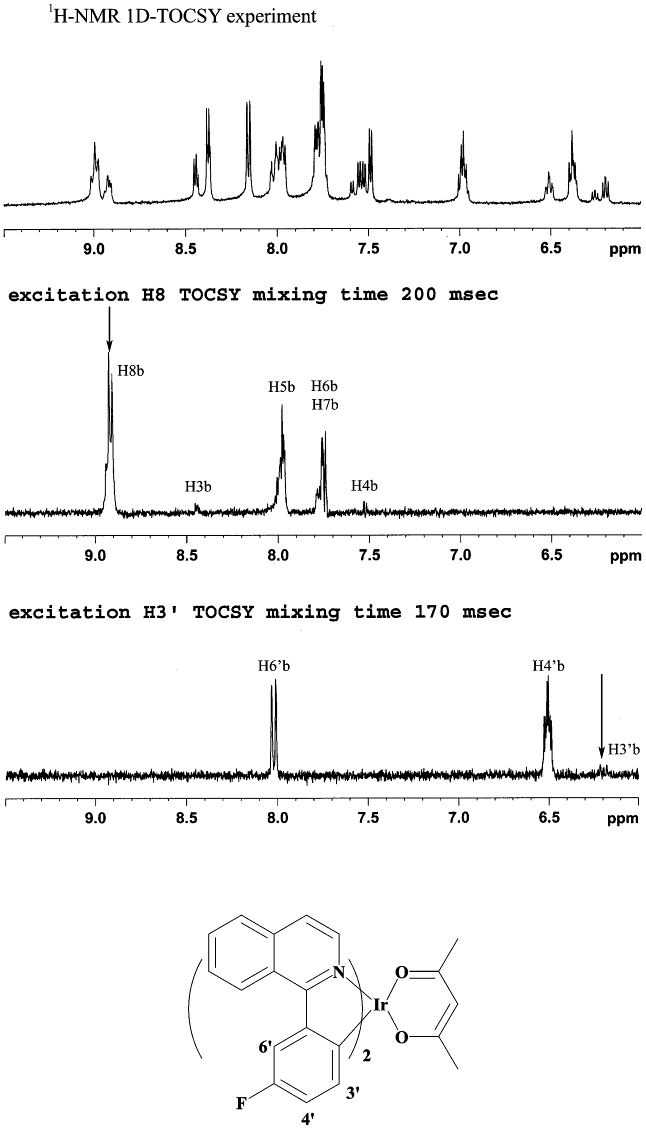

Figure 2. ^{1}H NMR 1D-TOSCY for (5′-fpiq)$_2$Ir(acac).

isomers could be obtained. Through TLC analysis, we found only one spot (R_f is 0.76) on the TLC plate. Subsequent ^{1}H NMR analysis using a 1D selective TOCSY experiment revealed that the spot contained 2′-coordinated (3′-fpiq) and 6′-coordinated (5′-fpiq) iridium complexes with isomer (3′-fpiq)$_2$Ir(acac) as the major product (as shown in Figures 1 and 2). The corresponding E_{rel} value for the $-$OCH$_3$-substituted piq ligand is reduced from 38 to 11.4 kJ/mol. These results are consistent with the experimental data considering (1) only the 6′-cordinated isomer is acquired for ligand **4a1** and (2) the 6′-coordinated isomer (major product) accompanied by the 2′-coordinated isomer has been observed for ligand **4a3**.

To obtain electronic (orbital-based) explanations, atomic charges and molecular orbital components of the iridium complexes have been analyzed. Calculated results show that the 2′-coordinated (3′-opiq)$_2$Ir(acac) exhibits more positive charge on the Ir metal and more negative charge on the coordination atom (C$^{2'}$) than those in the 6′-coordinated (5′-opiq)$_2$Ir(acac). Iridium 5d-orbital content mixed into the LUMO, corresponding to the metal-to-ligand back-donation, indicating that, for each pair of isomers (**6a1**−**6a4**), higher back-donation is evident for the 2′-coordination isomer. In other words, 2′-coordination is favored by the back-donation effect, shown by charge analysis (more positive metal and more negative coordination carbon) and the 5d-character of the LUMO. This can account for the reduced E_{rel} value for the **6a3** pair of isomers since the sterically disfavored 2′-coordination is largely counterbalanced by electronic effects. Consequently, both isomers of **6a3** were obtained and were richer in the 6′-coordinated isomer.

Since fluoro is smallest in size among the substituents under study, the 2′-coordinated Ir complex, (3′-fpiq)$_2$Ir(acac), was obtained as the major product. It is expected that electronic effects (vide supra) play a major role in the relative energies of the pair of isomers. The calculated energies show that, contrary to the other three pairs (**6a1**−**6a3**), the 2′-coordinated iosmer is lower in energy than the 6′-coordinated isomer by 12 kJ/mol. Single crystals of (3′-fpiq)$_2$Ir(acac) were obtained from CH$_2$Cl$_2$−hexane solutions. The crystal structure determined by X-ray diffraction analysis is shown in Figure 3. The corresponding crystallographic data and selected bond lengths and angles are summarized in Table 2 and Table 3. The crystallographic data for (3′-fpiq)$_2$Ir(acac) reported here have been deposited in the Cambridge Database: CCDC #294796. The results of the DFT-optimized structure for (3′-fpiq)$_2$Ir(acac) are summarized in Table 4 together with the measured experimental values. As can be seen in this table, the calculated bond lengths are very close to the measured values.

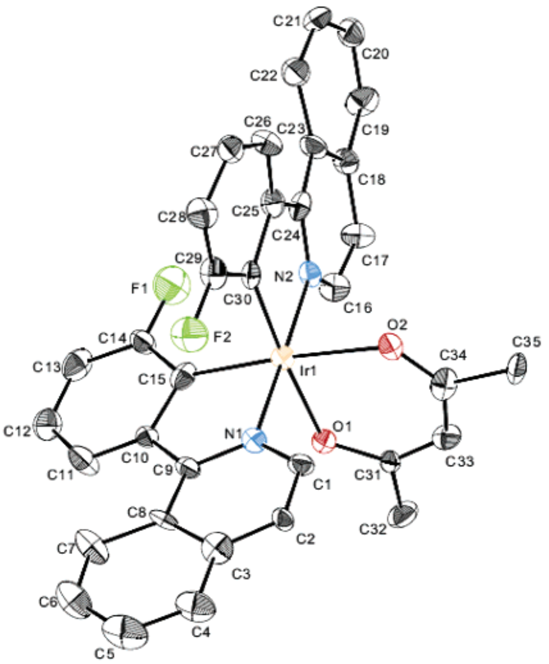

Figure 3. Diagram showing the molecular structure of (3′-fpiq)$_2$Ir(acac).

Table 4. Comparison of Calculated Bond Lengths and Experimental Values from X-ray Diffraction for (3′-fpiq)$_2$Ir(acac)

	calculation (Å)	experimental (Å)
Ir1−N1	2.07	2.053
Ir1−N2		2.045
Ir1−C15	2.01	1.993
Ir1−C30		1.988
C9−C10	1.47	1.47
C24−C25		1.48
C14−F1	1.36	1.33
C29−F2		1.34

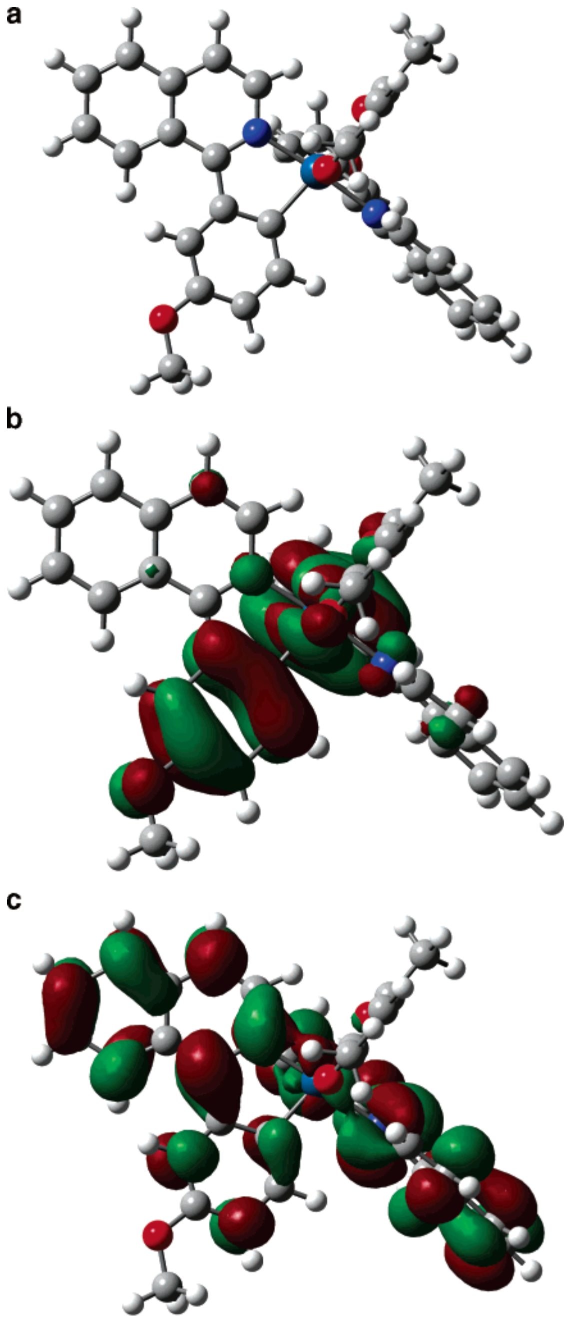

Figure 4. (a) Molecular structure of (5′-opiq)$_2$Ir(acac) (**6a3**). (b) Contour plot of the HOMO in **6a3**. (c) Contour plot of the LUMO in **6a3**. (Although the LUMO is mainly composed of the isoquinoline fraction of phenylisoquinoline, it also mixes with a little phenyl in character.)

Figure 4 shows contour plots of the highest occupied molecular orbital (HOMO) and the lowest unoccupied molecular orbital (LUMO) of (5′-opiq)$_2$Ir(acac) (**6a3**). The LUMO is mainly composed of an isoquinoline fraction of phenylisoquinoline, whereas the HOMO contains significantly the phenyl part of phenylisoquinoline besides the metal. Substitutions on the 5′-position of phenyl will directly affect the π-donating capability of the phenyl ring and consequently vary the energy of the HOMO. This is responsible for various luminescent frequencies observed for 5′-substituent = OCH_3 (**6a3**), CH_3 (**6a1**), and CF_3 (**6a2**) in the current study: methoxyl (a stronger donor) will tune the HOMO, leading to decreased band gaps compared with the methyl group (a weaker donor), as reported in “color tuning” studies.[4,12] On the basis of our calculated results for the trifluoromethyl-substituted complex, this σ- and π-withdrawing substituent[13] stabilizes both HOMOs to a larger extent than the LUMO (compared with the CH_3-substituted complex) and, hence, leads to an increased band gap. The energies of HOMOs, LUMOs, and band gaps of all complexes are summarized in Table 1 for comparison purposes. Interestingly, the band gaps of these 6′-coordinated complexes (or all 2′-coordinated complexes) are in the order **6a2** > **6a1** > **6a3**, as found experimentally.

The lowest triplet excited state (T_1) energies of the four iridium complexes calculated by TDDFT are also contained in Table 1. T_1 in each complex arises from HOMO to LUMO excitation. The calculated values suggest that the 2′-coordinated iridium complexes (**6a1**, **6a2**, **6a3**, and **6a4**) all exhibit a hypsochromic shift with respect to their isomers. These results agree satisfactorily with the experimental electroluminescence data, suggesting that TDDFT calculations can predict the emission behavior of iridium complexes.

---

[12] Kwon, T. H.; Cho, H. S.; Kim, M. K.; Kim, J. W.; Kim, J. J.; Lee, K. H.; Park, S. J.; Shin, I. S.; Kim, H.; Shin, D. M.; Chung, Y. K.; Hong, J. I. *Organometallics* **2005**, *24*, 1578.

[13] See reviews: (a) Wiberg, K. B.; Rablen, P.R. *J. Am. Chem. Soc.* **1993**, *115*, 614. (b) Schneider, W. F.; Nance, B. J.; Wallington, T. J. *J. Chem. Am. Soc.* **1995**, *117*, 478.

4. Conclusion

This study shows that density functional theory can be applied successfully for rationalizing the coordination behavior of the substituted phenylisoquinoline iridium complexes and the prediction of the emission of these complexes. This would facilitate the designing of new ligands for light-emitting iridium complexes.

Acknowledgment. This work was supported by the National Science Council of the Republic of China, Taiwan.

Supporting Information Available: X-ray crystallographic data, including a cif file for (3′-fpiq)$_2$Ir(acac), are available free of charge via the Internet at http://pubs.acs.org.

OM060323P